Z. Phys. B 96, 333–340 (1995)

ZEITSCHRIFT
FÜR PHYSIK B

Crystal-field induced dipoles in heteropolar crystals II: physical significance

Mario Birkholz

Ingenieurbüro für Solartechnik, Offenbacher Strasse 7, D-14197 Berlin, Germany

Received: 11 July 1994

Abstract. The significance of dipole moments induced by crystal fields in heteropolar crystals is discussed with respect to some aspects of solid state physics. Experimental results from structural analyses that provide data on induced dipoles are summarized. The concept of ionic radii is reconsidered, and a new tabulation scheme is proposed in terms of deformed charge distributions. It is shown that spontaneous polarization as well as the pyro- and piezoelectric coefficients are not independent sets of crystallographic constants, but are accounted for by the structural parameters, the ionic polarizabilities and the elastic constants. The dipole concept is extended to statistically induced or random dipoles. They can account for an important part of the binding energy of substitutionally disordered and non-stoichiometric compounds and, therefore, are concluded to stabilize disorder in solids.

PACS: 61.50.Lt; 77.60.+v; 77.70+a

Introduction

In part I of this work [1], in the following referred to as I, second-order electrostatic moments or dipoles were assigned to ions that reside on positions of certain symmetry in heteropolar crystals. Formulas for their calculation that makes use of the ions' polarizabilities and infinite lattice sums were given. The latter may be regarded as higher order Madelung constants. The significance of the dipole concept for the binding energy E_B was considered in I, where it was shown that a surplus addend is introduced in E_B, called polarization energy E_p. If dipole-dipole interactions become small enough to be neglected, E_p will always strengthen the crystal binding.

Important applications of the dipole model in condensed matter physics arose in connection with investigations of the dielectric function. For crystals with ions on cubic lattice sites, the Clausius-Mossotti relation is obtained for the limit of infinite frequencies, as was already found in the last century, and which was later explained by a theory of Lorentz that combined microscopic and macroscopic elements. In the following, important supplements for liquids with polarized and polarizable molecules were established by Debeye, Onsager and others, an extensive description of this path of dipole research is given in [2]. For crystals, Lorentz's approach was reformulated by Ewald and Born on a complete microscopic basis [3]. Only recently, an investigation of the magnetic birefringence in rutile-type antiferromagnets [4] concluded that "the classical point-dipole model, upon which the Ewald-Born theory is based, is considerably more powerful than is commonly assumed".

However, these applications of dipole models differ significantly from those presented in I in as much as they deal with dipoles that are induced by external fields. However, in I dipoles were considered that are caused by internal or crystal electric fields. Also, many investigations have been carried out with regard to this dipole conception. Part I citied some works that aimed at calculating the electrical field gradient at the nucleus of ions, which also included dipole terms. In addition, the different phases of ferroelectrics have been an important field for dipole models. In order to understand their cross section in neutron scattering, for instance, elastic dipole models that imagine the dipoles to be associated with certain ionic groups within the unit cell have been developed [5, 6].

It is again emphasized that the model as discussed in this work regards the dipoles to be localized at the ions themselves. They are assumed to be coupled to the ions' positions as is the crystal electrical field that induces them. Consequently, this will cause the moments to vanish as the solid melts or decomposes. Whereas molecules with permanent dipole moments (e.g. water) remain polarized during the transition from the solid to the liquid or the gase phase, this does not apply to the ionic dipoles discussed here. In this part of the work, further aspects of crystal-field induced dipoles will be considered that are relevant to some features of crystal physics.

Distribution of chemical elements over different lattice sites

Which ions can be found at positions allowing for dipole moments in the crystal? To answer this question it is recalled that the part of the binding energy due to the dipoles, the polarization energy E_p, can be formulated in terms of second-order Madelung constants α^d as

$$E_p = \frac{E_0}{2} \sum_{i=1}^{N} \sum_{j=1}^{M} \frac{K_i}{Z} z_i \mu_j \alpha_{ij}^d. \tag{1}$$

K_i stands for the frequency of i.th ions with a charge of $q_i = e z_i$. The crystallographic unit cell contains N sorts of ions, M different dipoles and Z formula units of the compound. The dipole strengths p_j are given in their normalised form, $\mu_j = p_j/ew$, with w being the cube root of the cell's volume V. E_0 is an energy unit, $E_0 = 2Ryd\, a_0/w$, and a_0 is Bohr's radius. α^d accounts for an inifinite lattice sum that describes the potential of all the j.th dipoles acting at the i.th ionic site, see (10b) in I for its definition.

The strength of the dipoles μ_j was shown to follow from the polarizabilities κ_j of the ions and lattice sums of the β^m- and β^d-type, which account for crystal electric fields of monopoles and dipoles. The set of the α^m, α^d, β^m and β^d will sometimes be named electrostatic lattice coefficients in the following. In many cases, the recursive induction of dipole strength by other dipoles is small compared with the induction by charges. The β^d coefficients may then assumed to become zero. In this approximation the dipole strength, now symbolized by ϕ_j to distinguish them from μ_j, is proportional to the β^m coefficients and the polarizability: $\phi_j = \kappa_j \beta_j^m / V$. Together with a relation between α^d and β^m coefficients that describes the equality of charge-dipole and dipole-monopole interaction (see (12) of I), (1) is reformulated

$$E_p \cong -\frac{E_0}{2} \sum_{j=1}^{M} \frac{L_j}{Z} \frac{\kappa_j}{V} (\beta_j^m)^2 \tag{2}$$

where L_j is the frequency of the j.th dipoles within the unit cell. It can be seen from eq. (2) that the system has two possibilities for minimizing its energy with respect to the dipoles. First, ions may be shifted to dipole-allowed positions where non-vanishing β^m coefficients occur. This is not the case for all 32 point symmetries that describe crystallographic lattice sites, but only for a subset of ten of them, see the table in I. Second, the binding energy is more enhanced the more polarizable the ions residing on dipole-allowed positions.

In the periodic system of elements the atomic polarizability increases within a period from right to left, and within a group from top to bottom [7]. For heteropolar crystals, however, one has to consider the polarizabilities of the ions and the distribution of charges among them. This latter point is governed by differences in electronegativity. Since the elements on the right are more electronegative than those on the left, the former will bear the negative charges. These surplus electrons cause the polarizability to increase, whereas the polarizability of the counter-ions is reduced by the depletion of electrons.

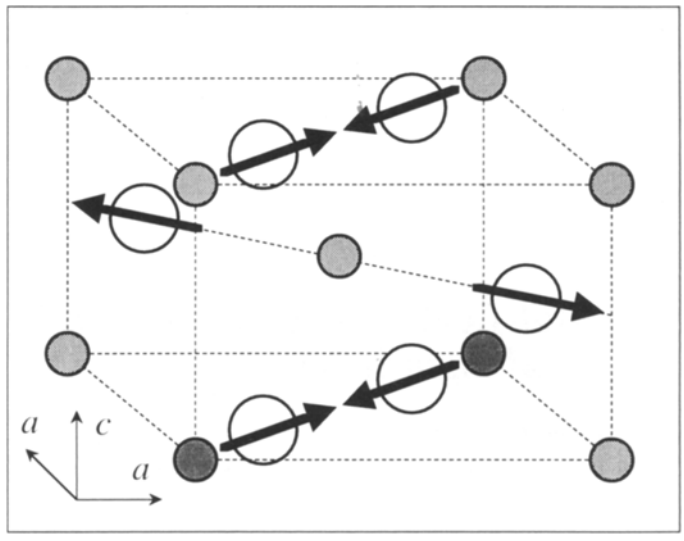

Fig. 1. Rutile-type structure (C4). White spheres symbolize oxygen ions, while grey spheres stand for titanium. Arrows should indicate dipole unit vectors

It is therefore the interplay between polarizability and electronegativity that determines the distribution of ions over different lattice sites. Consequently, one would expect the group V, VI and VII elements and the metals with large inner electron shells (i.e. lanthanides and actinides) to reside at positions, where crystal electrical fields may occur. Equation (2) provides the quantitative basis for that rule. The prediction is in agreement with many investigation done so far and with an inspection of crystal structures of binary compounds [8], where the more polarizable ion is always found to be situated on a dipole-allowed lattice site. Fig. 1 shows the rutile-type structure as a typical example in which dipole moments are induced at the oxygen lattice site.

Evidence for crystal field induced dipoles from diffraction experiments

There are two possibilities, by which charge distributions of ions may reveal a second-order electrical moment within the appropriate length scales of diffraction procedures. First, a displacement of the centroid of the negative charge distribution and the nucleus may be observed. Second, the square of the electronic wave function, which may be measured directly, is found to deviate from spherical symmetry. Diffraction experiments have given evidence for both phenomena in the case of polarizable ions on relevant lattice sites.

Before giving examples for the first effect, an upper limit for the spatial separation of the nucleus and the centroid of the electron cloud of an ionic dipole should be estimated. One may assume that the dipole is composed of two point charges, $p = (q_N + q_e) \times \Delta$, so the separation distance Δ can be estimated if p is known. This was done for the case of the oxygen ion [9] in TiO_2. Inserting $q_N = +8e$ and $q_e = -10e$ yields $\Delta = 0.08$ Å, which would be easy to detect in X-ray and neutron diffraction experiments that measure the center

Table 1. Structural parameters of some crystalline compounds in which dipole moments may occur on certain lattice sites. The positional parameters of the polarizable ions can be seen to differ according to the method by which they were determined. Whereas X- and γ-ray diffraction (XRD and GRD) reveal the centroid of the electron cloud, the neutron time-of-flight (N-TOF) method measures the position of the nucleus. The differences on an absolute scale are obtained by multiplying the figures with $1/\sqrt{3}a$ and $1/\sqrt{2}a$ for pyrite- and rutile-structures, respectively. The differences are very small but statistically significant

Compound	Structure, Cell Edges	Positional Paramter	Site Symm.	Measured Value	Method	Ref.
SiP_2	pyrite-type $a=b=c=$ 5.707 Å	$x(P)=y(P)$ $=z(P)$	C_3	0.39065(2) 0.39075(9)	XRD N-TOF	[10] [10]
MnF_2	rutile-type $a=b=4.874$ Å $c=3.310$ Å	$x(F)=y(F)$	C_{2v}	0.30523(7) 0.30503(5)	GRD N-TOF	[32] [11]
TiO_2	rutile-type $a=b=4.594$ Å $c=2.959$ Å	$x(O)=y(O)$	C_{2v}	0.30491(5) 0.30476(6)	XRD N-TOF	[13] [14]

of mass of the electron cloud and the position of the nuclei, respectively. But the approach does not concur with classical electrostatic arguments. When calculating the dipole strength with the help of this formula, it is normally presupposed that the two charges have no considerable overlap, which is by no means the case for the nucleus of charge q_N and the electron distribution of charge q_e. On the contrary, the nucleus is totally embedded within the electron cloud and the approach seems hardly reliable. Most probably, it can provide only an upper limit for the separation of the centers of mass of both charge distributions.

Differences between positional parameters as measured by electron-sensitive versus nuclei-sensitive diffraction procedures have been reported for (i) phosphorous [10] in SiP_2, (ii) fluorine [11, 12] in MnF_2 and (iii) oxygen [13–15] in TiO_2, see Table 1. The first compound crystallizes in the pyrite-structure, and the two latter in the rutile-structure, for the latter see Fig. 1. The observed differences are very small, being on the order of 10^{-3} Å. Indeed, they are much smaller than predicted by the approach $\Delta=p/(q_N+q_e)$ as discussed above. The positional parameters, however, differ significantly and it is concluded that they account for a true physical effect. This is corroborated by the fact that spatial separations are only observed for ions on dipole-allowed lattice sites, but are consistently absent if dipoles are forbidden due to local symmetry restrictions.

Also the second effect – the deviation from spherical symmetric charge distribution – can be verified by modern diffraction procedures. Routinely used computer programs allow for the calculation of ionic charge distribution as obtained from high-resolution single-crystal XRD in terms of spherical harmonics. Non-vanishing second-order moments of the electron distribution were obtained for many ions at dipole-allowed positions, e.g. for sulfur in FeS_2 [16], for phosphorous in SiP_2 [10], for fluorine in MnF_2 [12] and for oxygen in tetragonal $BaTiO_3$ [17], to mention only a few examples.

The dipolar deformation of charge distributions has an interesting and important effect on conventional X-ray structural analysis. For almost all structural refinements of intensity data gathered by X-ray diffraction, the utilized scattering factors were calculated for spherically symmetric atoms and ions [18, 19]. Such scattering factors will invariably lead to systematic error if applied to positions of ions for which the symmetry of the lattice site permits the occurrence of dipole moments. More reliable positional parameters will be obtained when the structural refinement is coupled with a refinement of the charge distribution. A comparision of both procedures is possible for the case of the polarizable S ion in pyrite, because the sulfur positional parameter u was measured by both methods [16, 20]. The difference is found to be as small as 2×10^{-4} in units of the cell edge a or 10^{-3} Å on an absolute scale, and the effect is concluded to be very small. Although this point involves huge amounts of crystallographic data in principle, it is probably significant only for high-precision work. However, the effect becomes very important when the spatial separation between the centroids of positive and negative charges of ionic dipoles is being measured..

These results imply that the crystal electrical field causes two different effects on ions at dipole-allowed lattice sites: (i) a difference between the nucleus' site and the controid of the electronic charge distribution and (ii) a deformation of the electron cloud. Although, this cannot be deemed an experimental determination of the dipole's strength, it evidences their occurrence.

The concept of crystal radii

Another consequence of dipole moments induced by crystal field concerns the concept of ionic radii, which is widely used in solid state science to estimate interionic distances in crystals. This concept approximates the charge distribution of an ion by reducing it to one geometric parameter, namely the radius of a sphere. It is evident that this approach needs to be generalised, if dipole-deformed charge distributions are to be associated with some ions. In such cases it would be more suit-

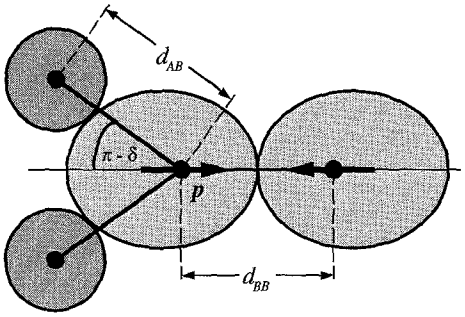

Fig. 2. Schematic drawing of chemical bonds as they may occur between ions A and B, with B bearing a dipole moment p. The interionic distance d depends upon the angle δ between the dipole p and the distance vector connecting both nuclei. Crystal radii r are proposed to be categorized by the parameters p and δ. This should improve the predictions of interionic distances in crystals

able to attribute the spatial extent of charge distributions to other geometrical objects, such as ellipsoids for instance. As can be seen in Fig. 2, it would be useful to characterize ionic radii r with two additional parameters: (i) the dipole strength, p, when applicable and (ii) the angle δ between the dipole vector and the interionic bond, abbreviated as $r(p, \delta)$. The geometrical conditions make it evident that these two parameters should provide comparable results for the same ion in different surroundings.

Consider for instance the sulfur ion, S^-, in FeS_2, which is bound to three Fe ions and one S ion. Its dipole strength was calculated [21] to be $0.77 e$Å or 12.3×10^{-30} Cm. The sulfur-sulfur bond d_{SS} of 2.15 Å [20] is oriented along the direction of the induced dipole, $\delta = 0$. Consequently, $r_S(0.77,0) = d_{SS}/2 = 1.08$ Å is obtained for S^-. The values for the Fe–S bond are $d_{FeS} = 2.26$ Å and $\delta = 102°$, but the value for the iron radius must now be specified. Since Fe ions reside on dipole-forbidden lattice sites, their usual ionic radius may be taken as obtained for the "spherical" ion by Pauling, $r_{Fe}(0,0) = 0.76$ Å, according to [22]. If the sum of iron and sulfur radii is assumed to equal the bond length, $r_S(0.77,102°) + r_{Fe} = 2.26$ Å, the second $r(p, \delta)$ value is obtained for the S^- ion, yielding $r_S(0.77,102°) = 1.5$ Å. This is much larger than the value obtained in direction of $\delta = 0$ as given above. It is concluded that electrons would have been depleted from the positive edge of the S-dipole and accumulated at the negative end. The result is consistent with the dipole model of S ions in pyrite [21].

The tables of ionic radii today normally in use represent only mean values obtained by averaging $r(p, \delta)$ over many p and δ. On the other hand, a tabulation scheme of all such $r(p, \delta)$ for each sort of ion would include second-order corrections, and would be more appropriate for predicting ionic distances in heteropolar crystals.

Spontaneous polarization and the pyroelectric coefficient

Crystal-field induced dipoles provide a particularly simple approach to describe electrically polarized crystals that have a macroscopic dipole moment without being subjected to an external field, i.e. pyroelectrics. Their dipole moment is specified per unit volume, and is called spontaneous polarization P_S. Theories on pyroelectricity often assume that the polarization is associated with the whole crystallographic unit cell or a certain molecular configuration within it. In the present approach, however, the ions on dipole-allowed lattice sites become the structural elements with which polarization is coupled. In the most general case, P_S is a vector with three different components. This can be expressed in terms of the developed notation as

$$\mathbf{P}_s = \sum_{j=1}^{M} L_j \frac{\mathbf{p}_j}{V} = \frac{e}{w^2} \sum_{j=1}^{M} L_j \mu_j \mathbf{n}_j = \frac{e}{w^2} \sum_{j,k=1}^{M} L_j B_{jk}^{-1} \beta_k^m \mathbf{n}_j \quad (3)$$

where $\boldsymbol{n}_j$ is the unit vector of the j.th dipole, and B_{jk} accounts for the polarizabilities κ_j and dipole-dipole interactions: $B_{jk} = \delta_{jk} V/\kappa_j - \beta_{jk}^d$.

Spontaneous polarization occurs only in certain crystal classes and on so-called polar axes. It is well known that the number of independent polar axes within the 32 crystal class is governed by the same distribution as the one given in the table in I. It can be seen from the table that for the compounds from crystal classes O_h, T_h, D_{4h} and D_{2h} discussed in the example section of I no spontaneous polarization occurs. In these solids, the sum over all dipole moments of the unit cell vanishes, although second-order moments are induced for some ions. However, for crystals belonging to the polar classes C_1, C_{1h}, C_{nv} and C_n, $n = 2, 3, 4, 6$, a macroscopically observable polarization may remain.

The fact that the sum of dipoles of the unit cell differs from zero only for polar crystal classes can be derived from the principle of superposition of symmetry or Curie's principle. According to it, the symmetry of a lattice site cannot be higher than the symmetry of the unit cell [23]. Consequently, the polar properties of the ions – as induced dipole moments, for instance – only become measurable quantities for polar crystal classes. It has to be mentioned, that a crystal belonging to one of the polar classes does not neccessarily have a spontaneous polarisation strong enough to be measured. However, all crystals for which a nonzero P_S is experimentally determined, belong to one of the polar classes.

The pyroelectric coefficient γ is the derivative of spontaneous polarization with respect to the temperature T. In general, γ is a three-component vector like P_S, but since most pyroelectrics have only one polar axis it may often be considered a scalar quantity. Equation (3) gives

$$\gamma = \frac{\partial \mathbf{P}_s}{\partial T} = \sum_{j,k} L_j \left[\left(\frac{\partial}{\partial T} \frac{e}{w^2} \right) B_{jk}^{-1} \beta_k^m + \frac{e}{w^2} \left(\frac{\partial B_{jk}^{-1}}{\partial T} \right) \beta_k^m + \frac{e}{w^2} B_{jk}^{-1} \left(\frac{\partial \beta_k^m}{\partial T} \right) \right] \mathbf{n}_j \quad (4)$$

The first term of (4) is found to be proportional to P_S

$$\left(\frac{\partial}{\partial T}\frac{e}{V^{2/3}}\right)\sum_{j,k} L_j B_{jk}^{-1}\beta_k^m \mathbf{n}_l$$
$$= -\frac{2}{3}\left(\frac{1}{V}\frac{\partial V}{\partial T}\right)\frac{e}{w^2}\sum_{j,k} L_j B_{jk}^{-1}\beta_k^m \mathbf{n}_j = -\frac{2}{3} Sp(\alpha)\mathbf{P}_s \qquad (5)$$

and the spur of the tensor of thermal expansion [24], $Sp(\alpha)$. When evaluating the third sum of (4), one must realize that electrostatic lattice sums depend upon the structural coordinates of the ions. If an ion is situated on a dipole-allowed lattice site, it is described by at least one free coordinate or structural parameter (in the case of spontaneously polarized, tetragonal $BaTiO_3$, these are, for instance, the oxygen and titanium deviations from their positions in the cubic phase [17]). The set of those parameters is symbolised by ζ_j. It is their temperature-dependence that enters the derivative of β_k^m

$$\frac{\partial \beta_k^m}{\partial T} = \sum_{j=1}^{M} \frac{\partial \beta_k^m}{\partial \zeta_j}\frac{\partial \zeta_j}{\partial T} \qquad (6)$$

The coefficients of the central term in eq. (4) become

$$\frac{\partial B_{jk}^{-1}}{\partial T} = -B_{jk}^{-2}\frac{\partial B_{jk}}{\partial T} = -B_{jk}^{-2}\left[\delta_{jk}\left(\frac{\partial}{\partial T}\frac{V}{\kappa_j}\right) - \frac{\partial \beta_{jk}^d}{\partial T}\right]. \qquad (7a)$$

If dipole-dipole interaction can be assumed to be insignificant, the inverse of B_{jk} is sufficiently approximated by $B_{jk}^{-1} = \delta_{jk}\kappa_j/V$. In contrast with (7a) it is obtained

$$\frac{\partial B_{jk}^{-1}}{\partial T} \cong \left[\frac{\partial \kappa_j}{\partial T} - \kappa_j Sp(\alpha)\right]\frac{\delta_{jk}}{V} \qquad (7b)$$

This approximation finally makes it possible to calculate the pyroelectric coefficient(s) γ using the formula

$$\gamma \cong -\frac{5}{3} Sp(\alpha)\mathbf{P}_s + \frac{e}{w^2}\sum_j L_j\left[\frac{\beta_j^m}{V}\frac{\partial \kappa_j}{\partial T} + \frac{\kappa_j}{V}\sum_k \frac{\partial \beta_j^m}{\partial \zeta_k}\frac{\partial \zeta_k}{\partial T}\right]\mathbf{n}_j \qquad (8)$$

The prefactor $-5/3$ in (8) as compared to $-2/3$ in (5) is caused by the occurrence of a factor $-3/3$ in (7b).

The pyroelectric coefficient splits into three different parts: $\gamma = \gamma_{ex} + \gamma_{pol} + \gamma_{pos}$. The first, γ_{ex}, is due to variations in the external lengths of the unit cell with temperature, i.e. thermal expansion. The third, γ_{pos}, is caused by changes in the positions of ions with increasing temperature. The second, however, accounts for modifications in the electronic structure that can significantly alter the ionic polarizabilities, γ_{pol}. The dipole-dipole interaction will have an influence on γ_{pos} only when further derivatives of the β^d sums enter the formula. Their inclusion is obvious from (7a) and similar to (6). Sometimes, the pyroelectric coefficient is defined to be the change of P_s with temperature at constant volume [24], which would abolish γ_{ex} from (8). In other cases, γ_{ex} is included in the definition [23], but it is said to account for pyroelectric effects of the second kind or pseudo-pyroelectric effects [25]. The terminology of pyroelectricity, unfortunately, is not uniform, and one must carefully verify which effect is actually being discussed.

One may therefore conclude that spontaneous polarization P_s and the pyroelectric coefficient γ are determined by atomic quantities as the polarizabilities, and such crystal properties as the electrostatic lattice sums and the tensor of thermal expansion. P_S and γ may be calculated if the structural parameters, their variation with temperature and the polarizabilities are known. Or, vice versa, the measurement of both quantities P_S and γ permits experimental determination of ionic polarizabilities κ_j and their temperature dependence.

In principle, it should be possible, to invert a polar axis of a pyroelectric crystal by applying an external electrical field. This must cause a displacement of ions within the unit cell, which is accounted for by mirroring the coordinates at a plane perpendicular to the polar axis, leading to $\zeta_j' = -\zeta_j$. Solids for which this is possible without destroying their crystal structure by the external field are known as ferroelectrics. The formulaes presented above should also account for their saturation polarization and the temperature dependence of the latter.

Piezoelectric coefficients

The ten polar classes are a subset of the 21 non-centrosymmetric crystal classes. Their unit cells lack a center of inversion, but the sum of dipoles which may occur must not necessarily deviate from zero. Directed forces as pressure or stress, are able to transform all non-centrosymmetric crystals into polar crystals (except for O or 432). Then an electric dipole moment may also occur for solids, which show no spontaneous polarization under force-free conditions. In polar crystals, the magnitude and direction of the macroscopic polarization as given by formula (3) is modified. This phenomena is well known as the direct piezoelectric effect. The piezoelectric constants $d_{i\lambda}$ are related to the external stress σ_λ and the induced polarization P_i through

$$P_i = d_{i\lambda}\sigma_\lambda. \qquad (9)$$

$d_{i\lambda}$ is a tensor having 18 independent components in the most general case. The index i now stands for the direction of polarization, which is induced or varied along one of the crystallographic axes a, b or c. The usual notation for σ_λ is used here, i.e. $\sigma < 0$ indicates a pressure and $\sigma > 0$ stands for stress, $1 \leqq \lambda \leqq 3$ accounts for forces perpendicular to the x-, y- or z-axis, and $4 \leqq \lambda \leqq 6$ stands for shear forces parallel to the planes. If there is more than one σ_λ acting upon the crystal, P_i becomes the sum over all non-zero products of $d_{i\lambda}\sigma_\lambda$.

To understand the piezoelectric effect in terms of the dipole concept, one should realize that, for $d_{i\lambda} \neq 0$, the unit cell is transformed into one of the polar classes. Depending on the crystal's symmetry and its orientation to the applied force, a new set of $\tilde{\beta}^m$ and $\tilde{\beta}^d$ values arises. Moreover, the point symmetry of formerly dipole-forbidden ionic positions may be reduced to become a dipole-

allowed lattice site. Both effects may cause the sum of dipoles $\tilde{\mu}$ of the unit cell to deviate from zero. The magnitude of the $\tilde{\beta}$ sums and crystal field induced dipoles $\tilde{\mu}$ depends upon the applied stress. These figures are marked by a tilde to distinguish them from those calculated in the force-free case. Consequently, it would be possible to calculate the $d_{i\lambda}$ if the atoms' coordinates for the crystal under pressure or stress were known.

The atom's coordinates, abbreviated by r, under ambient conditions are related to those under pressure, $\tilde{r}$, by the strain tensor e_{ij}

$$\tilde{r}=r+\sum e_{ij}r_i \tag{10}$$

that may be extracted from the inverse of Hooke's law

$$e_\nu=\sum S_{\nu\lambda}\sigma_\lambda \tag{11}$$

when the stress tensor σ_λ and the elastic constants $S_{\nu\lambda}$ are known. As usual in the theory of elasticity [26], the components of the symmetric strain tensor e_ν are numbered in (11) through ν, which is in agreement with the notation in (10) when $ij=xx,\ yy,\ zz,\ xy,\ xz,\ yz$ is inserted for $\nu=1,\ldots,6$. With their help the strained coordinates $\tilde{r}$ and the $\tilde{\beta}$ sums can be obtained according to (I, 10c, d). For the piezoelectric coefficients this finally yields

$$d_{i\lambda}=\frac{e}{w^2\sigma_\lambda}\left(\sum_{k=1}^{M} L_k\tilde{\mu}_k\mathbf{n}_k\right)_i=\frac{e}{w^2\sigma_\lambda}\left(\sum_{k,j} L_k\tilde{B}_{kj}^{-1}\tilde{\beta}_j^m\mathbf{n}_k\right)_i. \tag{12}$$

The meaning of the index i now is that only dipoles along the i-direction have be added. As for the pyroelectric coefficient, the formerly independent parameters $d_{i\lambda}$ become functions of coordinates of the atoms, charges and polarizabilities. In addition, the piezoelectric coefficients depend on the elastic constants $S_{\nu\lambda}$ that enter the induced dipole strength. The piezoelectric effect is normally assumed to scale linear with the applied stress within certain limits. It is emphasized that (12) allows for a more general prediction of $d_{i\lambda}$ as a function of σ_λ.

Randomly induced dipoles

Consider a crystalline model compound AC composed of positive ions A and negative C ions with charges z_A and $z_C=-z_A$. Both ions may reside on positions where crystal electric fields are forbidden and where no dipole moments are induced. Then, the A type ions are partially substituted by B ions of different valency $z_B\neq z_A$, and the solid solution $A_{1-x}B_xC$ is obtained. Both sorts of ions are assumed to occupy the same lattice site, being the A position of AC. A is then said to be heterovalently substituted by B. With a probability of $(1-x)$ one may find a charge z_A at that site, or with a complementary probability x one finds a charge z_B, i.e. the charges on A sites are accounted for by a two-point probability distribution [27]. If charges on former A and C sites are named z_1 and z_2, the mean value of z_1 now becomes $\overline{z_1}=(1-x)z_A+xz_B$. To preserve the charge neutrality of the crystal, the C ions have to be recharged, and their mean value becomes $\overline{z_2}=-\overline{z_1}$.

In many cases heterovalent substitutions are limited to certain solulability ranges of x. In the following it will be assumed that the incorporation of B ions neither alters the space group of the solid nor the point symmetry of the lattice sites (if A sites are assumed to be occupied by the new ionic species $A_{1-x}B_x$). Small deviations of the cell and positional parameters may occur due to differences in the geometrical appearance of A and B ions. $La_{2-x}Sr_xCuO_4$, which is orthorombic [28] for $T=10$ K and $0\leqq x\lesssim 0.21$, can be regarded as a recent example for such consideration.

The influence of statistically distributed charges on crystal electric fields and their associated dipoles should now be investigated. First, it has to be stated that, for a perfectly accidental distribution of A and B ions on A positions, the solid can no longer be named a crystal. A crystal is composed of a periodic array of repeated units and such a unit does not exist in the case of $A_{1-x}B_xC$. Approximately, the unit cell of AC with a "average ion" $A_{1-x}B_x$ on A positions may be regarded as the repeated unit. However, one can never certainly predict whether an A site will be occupied by an A or a B ion. Instead, one now deals with probability distributions. Thus, all properties of the solid that rely on the crystal structure will become statistically distributed quantities.

Concerning the question of induced dipoles, the symmetry of lattice sites as existing for $x=0$ vanishes or is disrupted. In a strict sense the point symmetry group of every lattice site becomes C_1 (1 in international notation) for $x\neq 0$, since all axes of rotation, mirror planes and centers of inversion disappear. This is caused by the fact that every arbitrarily selected ion may be surrounded by an asymmetric charge configuration of A and B ions with a finite probability. This leads to a crystal electric field, the strength of which varies over different lattice sites and which may induce varying dipole moments. For the i.th lattice site, the field's strength F_{ij} due to oher charges of the j.th type is described by the infinite lattice sum

$$F_{ij}=\frac{e}{4\pi\varepsilon_0}\sum_{j,j\neq i}\frac{z_j}{r_{ij}^2}=\frac{E_0}{ew}\sum_{j,j\neq i}\frac{z_j}{\rho_{ij}^2} \tag{13}$$

where the same notation as in I was used. The index j applies to all ions of the j.th type in the lattice. In the example of $A_{1-x}B_xC$, F_{21} accounts for the field of A and B ions at C lattice sites, $i=2$ and $j=1$. If both the A and C site are dipole-forbidden in accordance with the table in I, the average field vanishes

$$\overline{F_{ij}}=\frac{E_0}{ew}\sum_{j,j\neq i}\frac{z_j}{\rho_{ij}^2}=0. \tag{14}$$

But what will the mean of the square look like? To anser this question, one should remember that charges z_A and z_B are spread on A sites according to the rules

of a two-point distribution. In general, an infinite sum of a two-point distributed quantity yields a normal or Gauss distribution quantity [27]. Consequently, one would expect the F_{ij} to become normally distributed and to be entirely described by the first two statistical moments, i.e. average $\overline{F}_{ij}$ and variance $\sigma^2(F_{ij})$. Eq. (14) showed that the first moment $\overline{F}_{ij}$ equals zero in the case of the model compound $A_{1-x}B_xC$. Because it holds true for $\sigma^2(F_{ij})=\overline{F_{ij}^2}-(\overline{F}_{ij})^2$, the variance equals the mean square of the crystal field. The following calculation shows that the mean square field depends upon the statistical scatter of the j.th charge distributions $D^2(z_j)=\overline{z_j^2}-(\overline{z}_j)^2$, which is named dispersion in probability theory,

$$\begin{aligned}\frac{e^2w^2}{E_0^2}\overline{F_{ij}^2}&=\left(\sum_{j,\,j\neq i}\frac{z_j}{\rho_{ij}^2}\right)\left(\sum_{k,\,k\neq i}\frac{z_k}{\rho_{ik}^2}\right)=\sum_{j,k}\frac{\overline{z_jz_k}}{\rho_{ij}^2\rho_{ik}^2}\\&=\sum_j\frac{\overline{z_j^2}}{\rho_{ij}^4}+\sum_{j,k,\,j\neq k}\frac{\overline{z}_j\overline{z}_k}{\rho_{ij}^2\rho_{ik}^2}\\&=\sum_j\frac{\overline{z_j^2}}{\rho_{ij}^4}+\sum_{j,k}\frac{\overline{z}_j\overline{z}_k}{\rho_{ij}^2\rho_{ik}^2}-\sum_j\frac{\overline{z}_j^2}{\rho_{ij}^4}\\&=\sum_j\frac{\overline{z_j^2}-\overline{z}_j^2}{\rho_{ij}^4}=D^2(z_j)R_{ij}^4\end{aligned}\tag{15}$$

New infinite lattice sum, R_{ij}^4, has been introduced, and use has been made of the fact that the distribution of charges over one lattice site is not dependent on the distribution at other sites. The mean sum in the next to last line cancels according to (14). From (15) it can be concluded that the average square field is described by the dispersions of the two-point charge distributions. This result was to be expected, since both D^2 and σ^2 account for second moments of probability distributions and the variance of F_{ij} equals its mean square.

These considerations are only valid for ions on dipole-forbidden lattice sites as for the model compound $A_{1-x}B_xC$. It should be stated here without proof that in the case of dipole-allowed positions the mean sum in the next to last line of (15) would give cause for $(\beta_i^m)^2$ terms that would differ from zero on the i. position. Again, (15) would account for the equality $\overline{F_{ij}^2}=\sigma^2(F_{ij})+(\overline{F}_{ij})^2$, having this time $\overline{F}_{ij}\neq 0$.

The varying strength of crystal electrical fields will cause the ions to become polarized in a statistical manner. Like the crystal fields, the randomly induced dipoles will become normally distributed quantities with an average strength of zero. The effect of varying dipoles for the binding energy E_B of the solid becomes evident from the fact that the field strength enters into E_B according to $-pF/2=-4\pi\varepsilon_0\kappa F^2/2$. If disorder occurs in the solid, the binding energy will become a statistically distributed quantity also and its average $\overline{E_B}$ has to be considered. Then, nonvanishing terms $-4\pi\varepsilon_0\kappa\overline{F^2}/2$ arise and have to be included in the sum of terms of which E_B is composed of. Therefore, statistically induced dipoles supply a non-vanishing share to E_B although their average vanishes. To distinguish these disorder-related dipoles from the symmetry-restricted dipoles as introduced in I, they will be named random and regular dipoles, respectively. The strength of random dipoles may be identified with the square root of $(4\pi\varepsilon_0\kappa)^2\overline{F^2}$.

With the help of the formulas given above the share of the binding energy due to random dipoles $E_{p,ran}$ is found to be

$$\begin{aligned}E_{p,ran}&=-4\pi\varepsilon_0\sum_{i=1}^{N}\frac{K_i}{Z}\sum_{j=1}^{N}\frac{\kappa_i\overline{F_{ij}^2}}{2}\\&=-\frac{E_0}{2}\sum_{i,j=1}^{N}\frac{K_i}{Z}\frac{\kappa_i}{V}D^2(z_j)R_{ij}^4\end{aligned}\tag{16}$$

which stands for a new type of polarization energy in solids. Also $E_{p,ran}$ can be seen to be always negative. Its strength increases with increasing disorder according to the dispersion $D^2(z)$ of the charge distributions that reaches its maximum at the point of maximum disorder.

It has been argued in I that five regular dipole moments occur for orthorhombic $LaCuO_4$. Moreover, in the case of the high-T_c superconducting compound $La_{2-x}Sr_xCuO_4$, varying crystal electric fields arise on all four ionic sites. This may enhance the binding energy significantly. The occurrence of random dipoles likely is an important characteristic of all HTSC cuprates, since for them certain ions are generally found to be heterovalently substituted. Details of the calculation of $\sigma^2(F_{ij})$ for $La_{2-x}Sr_xCuO_4$ will be presented in a forthcoming work [29].

It still should be pointed to the fact, that the concept of statistically induced dipoles will also be relevant for defect structures. The generation of vacancies in crystal lattices is often accompanied by a redistribution of charges among the ions. In non-stoichiometric $Fe_{1-x}O$, for instance, the iron deficit causes a 3+ charge on some Fe ions in contrast to the normal 2+ charge of Fe in FeO [30]. One then has to calculate the binding energy of $(Fe^{3+})_{2x}(Fe^{2+})_{1-3x}O$, with the induced dipoles acting as stabilising factor of the stoichiometry-deviation. The same line of argumentation can probably be applied to sulfur-deficient pyrite [31], FeS_{2-x}, and many other compounds with strong stoichiometry deviations. It seems, that random dipoles provide an important mechanism for stabilizing disorder in crystals.

Conclusions

The significance of polarized ions was discussed for some aspects of solid state science. The displacement of centers of mass of the nucleus and the electron cloud and corroborating experimental results were shown. A new scheme for tabulating crystal radii in terms of dipole strength and orientation was proposed. Although it will be a laborious task to calculate and collect the necessary large number of $r(p,\delta)$ values, such a table would enable the calculation of more precise interionic distances. The state of crystal modelling is expected to improve significantly by the approach, leading to much better predictions of crystal structures by numerical simulations. The strength

of spontaneous polarization of macroscopically polarized crystals and the pyroelectric coefficient can be calculated if structural data and ionic polarizabilities are known. The same results were obtained for piezoelectric coefficients if the elastic constants of the compound are known also. Newly introduced random dipoles that arise in heterovalently substituted compounds were shown to increase the binding energy. This may be an important mechanism in the stabilisation of disorder in solids. I would expect that induced dipoles are of relevance for even more properties of crystalline solids. This work addressed only a few of them, which may be regarded as a preliminary selection.

I would like to thank R. Rudert, Max-Planck-Institut für Kolloid- und Grenzflächenforschung, D. Haase, Institut für Physikalische und Theoretische Chemie, I. Peschel, Institut für Theorie der kondensierten Materie, all in Berlin, and M. Schmitz, hydronic GmbH, Bitburg, for very helpful discussions and their support of this work.

References

1. Birkholz, M.: Z. Phys. B **96**, 325 (1995)
2. Böttcher, C.J.F., Belle, O.C. v., Bordewijk, P., Rip, A.: Theory of electric polarization, Vol. I & II. Amsterdam: Elsevier 1973 and 1978
3. Born, M., Goeppert-Mayer, M.: In: Handbuch der Physik, p. 623ff. Geiger, H., Scheel, K. (eds.) Berlin: Springer 1933
4. Jauch, W.: Phys. Rev. B**44**, 6864 (1991)
5. Schotte, U., Graf, H.A., Dachs, H.: J. Phys.: Condens. Matter **I**, 3765 (1989)
6. Schotte, U., Kabs, M., Dachs, H., Schotte, K.D.: J. Phys.: Condens. Matter **4**, 9283 (1992)
7. Miller, T.M., Bederson, B.: In: Advances in atomic and molecular physics, p. 1. Bates, D.R., Bederson, B. (eds.) New York: Academic Press 1977
8. Wyckoff, R.W.G.: Crystal structures, Vol. 1. New York: Interscience 1963
9. Bertaut, E.F.: J. Phys. (Paris) **39**, 1331 (1978)
10. Chattopadhyay, T.K., Schnering, H.G. v.: Z. Kristallogr. **167**, 1 (1984)
11. Jauch, W., Schultz, A.J., Heger, G.: J. Appl. Crystallogr. **20**, 117 (1987)
12. Jauch, W., Schultz, A.J., Schneider, J.R.: J. Appl. Crystallogr. **21**, 975 (1988)
13. Gonschorek, W.: Z. Kristallogr. **160**, 187 (1982)
14. Burdett, J.K., Hughbanks, T., Miller, G.J., Richardson, J., Smith, J.V.: J. Am. Chem. Soc. **109**, 3639 (1987)
15. Howard, C.J., Sabine, T.M., Dickson, F.: Acta Crystallogr. B**47**, 462 (1991)
16. Stevens, E.D., DeLucia, M.L., Coppens, P.: Inorg. Chem. **19**, 813 (1979)
17. Buttner, R.H., Maslen, E.N.: Acta Crystallogr. B**48**, 764 (1992)
18. Cromer, D.T., Mann, J.B.: Acta Crystallogr. A**24**, 321 (1968)
19. Cromer, D.T., Liberman, D.: J. Chem. Phys. **53**, 1891 (1970)
20. Finklea, S.L., Cathey, L., Amma, E.L.: Acta Crystallogr. A**32**, 529 (1976)
21. Birkholz, M.: J. Phys.: Condens. Matter **4**, 6227 (1992)
22. Cotton, F.A., Wilkinson, G.: Advanced inorganic chemistry, p. 52. New York: Wiley 1972
23. Zheludev, I.S.: Kristallphysik und Symmetrie, pp. 26 and 150. Berlin: Akademie-Verlag 1990
24. Kleber, W., Bautsch, H.-J., Bohm, J., Kleber, I.: Einführung in die Kristallographie, pp. 249 and 262. Berlin: Verlag Technik 1990
25. Tichy, J., Gautschi, G.: Piezoelektrische Meßtechnik, p. 76. Berlin: Springer 1980
26. Weißmantel, C., Haman, C.: Grundlagen der Festkörperphysik, Chap. 5.1. Berlin: VEB Deutscher Verlag der Wissenschaften 1989
27. Fisz, M.: Wahrscheinlichkeitsrechnung und mathematische Statistik, p. 160, Chap. 6. Berlin: VEB Deutscher Verlag der Wissenschaften 1980
28. Takagi, H., Cava, R.J., Marezio, M., Batlogg, B., Krajewski, J.J., Peck, W.F., Bordet, P., Cox, D.E.: Phys. Rev. Lett. **68**, 3777 (1992)
29. Birkholz, M., Rudert, R.: Z. Phys. B (in preparation)
30. Goodenough, J.B., Hamnett, A.: In: Landolt-Börnstein – Zahlenwerte aus Naturwissenschaften und Technik, Madelung, O., Schulz, M., Weiss, H. (eds.) Vol. 17g, p. 208. Berlin: Springer 1984
31. Fiechter, S., Birkholz, M., Hartmann, A., Dulski, P., Giersig, M., Tributsch, H., Tilley, R.J.D.: J. Mat. Res. **7**, 1829 (1992)
32. Jauch, W., Schneider, J.R., Dachs, H.: Solid State Commun. **48**, 907 (1983)